BULLETIN OF THE POLISH ACADEMY OF SCIENCES
TECHNICAL SCIENCES, Vol. 70(4), 2022, Article number: e142050
DOI: 10.24425/bpasts.2022.142050

A computationally low burden MPTC of induction machine without prediction loop and weighting factor

Babak KIANI*

Department of Electrical Engineering, Izeh Branch, Islamic Azad University, Izeh, Iran

Abstract. This paper presents a novel method to overcome problems of finite set-model-based predictive torque control (MPTC) which has received a lot of attention in the last two decades. Tuning the weighting factor, evaluating a large number of switching states in the loop of the predictive control, and determining the duty cycle are three major challenges of the regular techniques. Torque and flux responses of deadbeat control have been developed to overcome these problems. In our method, firstly, the prediction stage is performed just once. Then, both the weighted cost function and its evaluation are replaced with only simple relationships. The relationships reduce torque ripple and THD of stator current compromisingly. In the next step, the length of the virtual vector is used to determine the duty cycle of the optimum voltage vector without any additional computations. The duty ratio does not focus on any relation or criteria minimizing torque or flux ripple. As a result, torque and flux ripples are reduced equally. The proposed duty cycle is calculated by using a predicted virtual voltage vector. Hence, no new computation is needed to determine the proposed duty cycle. Simulation and experimental results confirm both the steady and dynamic performance of the proposed method in all speed ranges.

Key words: MPTC; induction motor; duty ratio; voltage vector; look-up table; weighting factor.

1. INTRODUCTION

In recent years, MPTC has been frequently investigated in controlling electrical torque and stator flux of electrical machines. MPTC has been accepted in the industry due to the prediction of the behavior of electric drive and considering the various constraints, objectives, and direct selection of inverter voltage vectors. As the first step of this technique, the torque and stator flux must be estimated. Then, electrical torque and stator flux are predicted by substituting all real voltage vectors of the inverter in a motor model. In the next step, the predicted variables are evaluated in a cost function. Finally, the voltage vector leading to the lowest cost is selected as an optimum voltage vector and applied to the motor.

This strategy suffers from major drawbacks such as the high computational burden of the processor and the challenge of the weighting factor determination. MPTC-based algorithms can be divided into two categories: one-vector-based and duty-cycle-based MPTCs (Duty-MPTC). Several types of one-vector-based MPTC algorithms have been presented in [1–7]. In [5], an optimum weighting factor has been calculated based on torque ripple minimization. The weighting factor is achieved by a complicated solution. It varies with the change of operating point. To overcome the challenge of weighting factor tuning, without weighting factor techniques have been presented in [8–13]. In [8], a ranking-based MPTC is presented to eliminate the weighting factor of the cost function. Since the ranking of torque and flux errors is a time-consuming process, this technique does not work properly in multilevel converters. Sequential-based MPTC algorithms are introduced in [9, 10]. Although the challenge of weighting factor determination is eliminated, the execution time of the prediction loop is twice as long as the traditional MPTC. In [11], the term stator flux has been separated from the cost function and replaced by a hysteresis band. However, this strategy leads to the challenge of hysteresis band determination. Using homogenous terms in the cost function is another way to eliminate the weighting factor that is presented in [12]. In this strategy, reference currents of a field-oriented algorithm have been compared to predicted current, which is calculated in a reference frame of the rotor flux. The drawbacks of this method are the diminishing of dynamic response and increasing the computational burden.

Computational burden reduction of MPTC has been investigated in [11,14–16]. In [11,14] the number of candidate voltage vectors is reduced. But determining the flux position for identifying the candidate voltage vectors takes a long time. In [15], candidate voltage vectors are selected based on a continuous deadbeat solution of torque and flux. Although the number of candidate voltage vectors is reduced, the execution time of an algorithm is high due to the high computational burden of continuous deadbeat response.

Further reduction of torque and flux ripples is achieved by employing Duty-MPTC. In this category of torque and flux control methods, a zero-voltage vector along with one or two active voltage vectors is applied to the motor at each control period. Some of these techniques have been studied in [17–20]. Since the lowest ripples of both torque and flux are not obtained only

*e-mail: babakk_kianii@yahoo.com

Manuscript submitted 2022-05-25, initially accepted for publication 2022-06-29, published in August 2022.

by applying two voltage vectors, all of these strategies have focused on torque ripple reduction. This goal is achieved by different criteria such as minimum torque ripple, torque deadbeat response, etc. However, a high level of flux ripple leads to a high value of THD current.

In [21], an algorithm is presented to tackle this problem. In this technique, firstly, the MPTC algorithm extracts the optimum voltage vector. Then, the optimum time of the voltage vector is determined based on the lowest torque error criteria. However, cascade determination of voltage vector and duty cycle causes weak operation, especially at low-speed ranges. To tackle the successive determination of the optimum voltage vector and its respective duty ratio, simultaneous selection of them has been studied in [22-24]. The calculated duty ratios and feasible voltage vectors are evaluated in the prediction loop. However, the calculated duty ratio has the disadvantages of parameter dependence as well as a high computational burden. The paper [24] introduces a similar technique that considers 25 combinations of voltage vectors to test. In addition, parameter dependence and a high processing time of the prediction loop are other disadvantages of this method.

Three vector-based MPTCs are the last efforts to reduce both torque and stator flux, and some of these algorithms are presented in [25, 26]. Although torque ripple and THD current are significantly decreased in these techniques, intensive derivation cannot be avoided.

In this paper, by calculating torque and flux deadbeat response, not only prediction stage is done just once but also real and imaginary components of calculated response are utilized as command values of the control system. These values are compared with real and imaginary components of inverter voltage vectors. So, the challenge of weighting factor tuning is removed. Also, the duty ratio is determined directly and without further calculations by using the deadbeat response. The proposed duty ratio does not consider any criteria over torque or flux response. Hence, both torque and flux ripples are equally reduced.

Other parts of this paper are summarized as follows:

The system has been modelled in Section 2. The principle of the proposed method has been explained in Section 3. Simulation and experimental results are presented and discussed in Sections 4 and 5, respectively.

2. MODELS OF INDUCTION MOTOR AND 2L–VSI

The dynamic model of the multi-phase induction machine in the stationary reference frame and in terms of space vector variables is expressed based on two electrical and one mechanical equation as follows:

$$\frac{\mathrm{d}\vec{\psi}_s}{\mathrm{d}t} = \vec{V}_s - R_s\vec{I}_s\,, \tag{1}$$

$$\frac{\mathrm{d}\vec{\psi}_r}{\mathrm{d}t} = R_r\vec{I}_r - j\omega_r\vec{\psi}_r\,, \tag{2}$$

$$\frac{\mathrm{d}\omega_r}{\mathrm{d}t} = \frac{P}{2J}\left(T_e - T_m\right), \tag{3}$$

where the variables of $\vec{I}_s$, and $\vec{I}_r$ are the space vectors of stator and rotor currents, respectively, and ω_r is the electrical speed of the rotor. Meanwhile, the parameters R_s and R_r are the stator and rotor resistances, respectively. Also, parameters J and P in the mechanical equation are the moment of inertia and the number of poles, and T_m is the torque of mechanical load. Also, $\vec{V}_s$ is the stator voltage vector.

In equations (1)–(3), $\vec{\psi}_s$, $\vec{\psi}_r$ and T_e are the stator flux, rotor flux, and inducted torque, respectively. These variables are expressed based on three algebraic equations:

$$\vec{\psi}_s = L_s\vec{I}_s + L_m\vec{I}_r\,, \tag{4}$$

$$\vec{\psi}_r = L_m\vec{I}_s + L_r\vec{I}_r\,, \tag{5}$$

$$T_e = \frac{3P}{4}\Im m\left(\vec{I}_s\vec{\psi}_s^{\,*}\right), \tag{6}$$

where parameters L_m, L_s and L_r are the mutual, stator, and rotor inductances, respectively.

$\vec{V}_s$ in equation (1) is provided by a 2L–VSI and can be presented as follows:

$$\vec{V}_s = (t_i/T_s)\vec{V}_s^{\,i}, \tag{7}$$

where $i = 1,\ldots,6$ and $\vec{V}_s^{\,i}$ are the basic voltage vectors of the 2L–VSI. t_i is the duration time of the applied voltage vector $\vec{V}_s^{\,i}$ and T_s is the sampling time

$$\vec{V}_s^{\,i} = \frac{2}{3}V_{dc}\exp\left(j\frac{\pi}{3}(i-1)\right). \tag{8}$$

In addition to six active voltage vectors, two zero voltage vectors, namely $\vec{V}_0$ and $\vec{V}_7$ can be generated by the 2L–VSI.

3. THE PRINCIPLE OF THE PROPOSED METHOD

High switching frequency, use of rotary reference frame, and modulator employment are the drawbacks of deadbeat (three vectors based) torque and flux control techniques. However, these methods have the lowest torque and flux ripples, and this response has other three excellent properties. Firstly, with the obtained response, the cost function evaluation stage is only performed for voltage vectors located in the vicinity of this response. The proposed evaluation is done with a simple lookup table. Meanwhile, a presented lookup table is formed based on the distances of the achieved virtual voltage vector from the actual voltage vectors of an inverter. On the one hand, this process relieves MPTC based method from the weighting factor tuning problem, and on the other hand, a comparison of homogenous terms, i.e. reference voltage and feasible voltage vectors, achieves a tradeoff between torque and flux ripples. Finally, the length of the virtual voltage vector has been utilized to determine the duty ratio in two vector-based algorithms with a simple relationship. In this paper, combinatorial methods of continuous and discrete MPTC have been presented.

3.1. Estimation of motor variables

In order to avoid dc offset or drift in a simple estimator and to have a robust observation, a sliding mode full order observer

has been presented in [27]. It is employed to calculate control variables in this paper.

After estimating $\vec{I}_s^{k+1}$ and $\vec{I}_r^{k+1}$ by employing the mentioned observer, rotor and stator flux, as well as electrical torque, are calculated as follows:

$$\vec{\psi}_s^{k+1} = L_s\vec{I}_s^{k+1} + L_m\vec{I}_r^{k+1}, \tag{9}$$

$$\vec{\psi}_r^{k+1} = L_m\vec{I}_s^{k+1} + L_r\vec{I}_r^{k+1}, \tag{10}$$

$$T_e^{k+1} = \frac{3P}{4}L_m\Im m\left(\vec{I}_s^{k+1}\cdot\vec{I}_r^{k+1*}\right). \tag{11}$$

where k is the next sampling time.

3.2. The proposed one-vector-based MPTC algorithm

A key point of the proposed strategy is the predicting of a virtual voltage vector being the reference voltage vector of torque and flux deadbeat solution. In this way, the optimum virtual voltage vector of torque and flux deadbeat control in a stationary reference frame is used as a starting point of the MPTC algorithm. In discrete control and for a deadbeat solution, control variables must be equal to their references at the end of each sample period. These conditions are given as follows in [28]:

$$T_e^{\text{ref}} = T_e^{k+2}, \tag{12}$$

$$\vec{\psi}_s^{\text{ref}} = \vec{\psi}_s^{k+2}. \tag{13}$$

On the other hand, dynamic equations of electrical torque and stator flux related to induction motor in discrete and scaler form are stated as follows in [28]:

$$\frac{\vec{\psi}_s^{k+2} - \vec{\psi}_s^{k+1}}{T_s} \approx \vec{v}_s, \tag{14}$$

$$\begin{aligned}\frac{T_e^{k+2} - T_e^{k+1}}{T_s} \approx & -T_e^{k+1}\lambda\left(R_rL_s + R_sL_r\right)\\ & - a_T\omega_r^{k+1}\left(\psi_{sd}^{k+1}\psi_{rd}^{k+1} + \psi_{sq}^{k+1}\psi_{rq}^{k+1}\right)\\ & + a_T\left(v_q^{k+1}\psi_{rd}^{k+1} - v_d^{k+1}\psi_{sq}^{k+1})\right),\end{aligned} \tag{15}$$

where $\lambda = \dfrac{1}{L_rL_s - L_M^2}$ and $a_T = \dfrac{3}{2}\dfrac{p}{2}\lambda L_M$.

By solving equations (14) and (15) simultaneously v_q^{k+1} can be achieved and is named v_q^{ref}:

$$\begin{aligned}v_q^{\text{ref}} = & \left(\left(T_e^{\text{ref}} - T_e^{k+1}\right)/T_s - T_e^{k+1}\lambda\left(R_rL_s + R_sL_r\right)\right.\\ & + a_T\omega_r^{k+1}\left(\psi_{sd}^{k+1}\psi_{rd}^{k+1} + \psi_{sq}^{k+1}\psi_{rq}^{k+1}\right)\\ & \left. + a_T\alpha\psi_{rq}^{k+1}\right)/\left(a_T\left(\psi_{rd}^{k+1} - \beta\psi_{rq}^{k+1}\right)\right),\end{aligned} \tag{16}$$

also v_d^{k+1} with a new symbol, v_d^{ref} is presented as

$$v_d^{\text{ref}} = \alpha + \beta v_q^{\text{ref}}, \tag{17}$$

where α and β are stated as follows:

$$\begin{aligned}\alpha = & \left(\left(\psi_s^{\text{ref}}\right)^2 - \left(\left|\vec{\psi}_s^{k+1}\right|\right)^2 + 2\psi_{sq}^{k+1}I_{sq}^{k+1}T_s\right.\\ & \left. + 2\psi_{sd}^{k+1}I_{sd}^{k+1}T_s\right)/(2\psi_{sd}^{k+1}T_s),\end{aligned} \tag{18}$$

$$\beta = -\psi_{sq}^{k+1}/\psi_{sd}^{k+1}. \tag{19}$$

In the proposed strategy, not only prediction is performed only once, but also the stage of candidate voltage vector selection does not exist. As a result, the computational burden of the proposed method is reduced significantly.

The evaluation of the cost function for the obtained candidate voltage vectors is the last part of the MPTC-based algorithm. In the MPTC, the cost function is used to find the optimal voltage vector among the candidate ones. The cost function can be included in some terms. Tracking of torque and also flux are the major terms of the cost function.

In this paper, instead of a total enumeration of all feasible voltage vectors in an evaluation loop, only the closest voltage vector to the virtual voltage will be directly selected. This selection process is conducted with a simple lookup table instead of candidate voltage vector selection and cost function evaluation processes. Hence, cost function evaluation and weighting factor tunning problems are simultaneously eliminated, the computational burden of the MPTC algorithm is significantly reduced, and torque and flux ripples are equally reduced. The algorithm of optimum voltage vector selection is presented below:

$$R_v = \left|v_q^{\text{ref}}/v_d^{\text{ref}}\right|, \tag{20}$$

$$s_{vd} = \text{sign}\left(v_d^{\text{ref}}\right), \tag{21}$$

$$s_{vq} = \text{sign}\left(v_q^{\text{ref}}\right), \tag{22}$$

if $\left|\vec{v}_s^{\text{ref}}\right| > V_{dc}/3$,

$$\text{if } R_v > 0.5 \quad \vec{V}_s^{\text{opt}} = 0.5s_{vd}vdc + 0.5\sqrt{3}s_{vq}vdc, \tag{23}$$

$$\text{if } R_v < 0.5 \quad \vec{V}_s^{\text{opt}} = (2/3)s_{vd}vdc \tag{24}$$

else

$$\text{if } \left|\vec{v}_s^{\text{ref}}\right| < V_{dc}/3 \quad \vec{V}_s^{\text{opt}} = 0. \tag{25}$$

Finally, $\vec{V}_s^{\text{opt}}$ is extracted as an optimum voltage vector and applied to the motor. The overall control diagram of the proposed algorithm has been shown in Fig. 1.

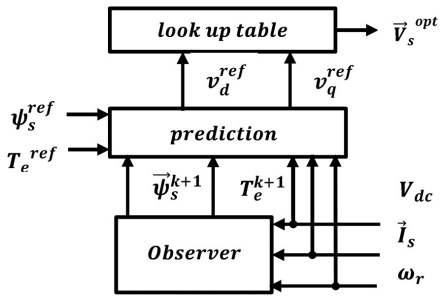

Fig. 1. The control diagram of the proposed FS-MPTC

3.3. The proposed duty ratio based on FS-MPTC

Although in the previous section electrical torque and stator flux were properly controlled by applying a single voltage vector at each sampling time, the torque and flux ripples are still very high. Applying a zero-voltage vector along with active voltage vectors at each sampling time reduces torque and flux ripples severely. This technique is known as the duty-ratio-based method. The duty ratio can be defined as the absolute value of the command voltage vector divided by the magnitude of the basic voltage vectors of an inverter. So, the ratio of voltage magnitude derived from the deadbeat response to the magnitude of basic voltage vectors is one of the best values that can be introduced as the duty ratio. The related diagram has been shown in Fig. 2.

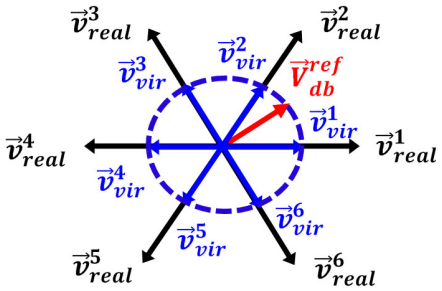

Fig. 2. Duty cycle determination in the proposed method

This diagram shows both real and virtual voltage vectors nominated $\vec{v}^i_{\text{real}}$ and $\vec{v}^i_{\text{vir}}$. In this figure, $\vec{v}^i_{\text{real}}$ are basic voltage vectors of a two-level inverter and $\vec{v}^i_{\text{vir}}$ are the virtual voltage vectors obtained from the duty ratio of the deadbeat solution. The duty ratio of the torque and flux deadbeat solution is named dr_{db}. By considering the presented diagram and stated points, the duty ratio is calculated as

$$dr_{db} = \left|\vec{V}^{\text{ref}}_{db}\right| / \left|\vec{V}^{i}_{\text{real}}\right|, \tag{26}$$

where $\vec{V}^{\text{ref}}_{db}$ is the output of the continuous deadbeat controller. Since the magnitude of basic voltage vectors is $2V_{dc}/3$, the duty ratio corresponding to the deadbeat solution will be calculated as follows:

$$dr_{db} = \left|\vec{V}^{\text{ref}}_{db}\right| / (2V_{dc}/3)\,. \tag{27}$$

This duty ratio has been calculated. The answer is the same as the dead response of the continuous torque and flux. Finally, the duration time of the selected voltage vector is determined as follows:

$$t_{\text{on}} = dr_{db} T_s\,. \tag{28}$$

As shown in this relation, the duty ratio is calculated only by using the virtual voltage vector obtained in the deadbeat solution, and other complicated computations are not required. The main advantage of the proposed duty ratio is that the output voltage of the aforementioned method takes into account deadbeat responses of both torque and flux simultaneously. So, the proposed duty cycle reduces the ripples of both the electrical torque and stator flux and not just one of them. In fact, in the two-vector-based method, it is not possible to provide the deadbeat response for both torque and flux at the same time. Hence, the deadbeat response of three-vector-based predictive control is an appropriate alternative for two-vector-based methods to satisfy a compromised level of ripples for electrical torque and stator flux. This mechanism has been illustrated in Fig. 3.

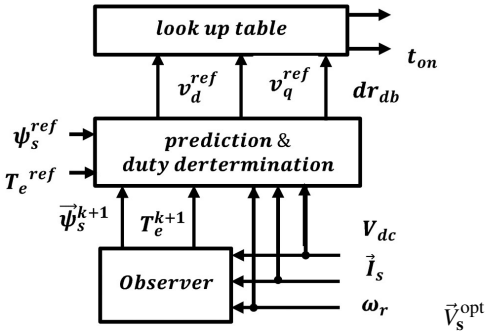

Fig. 3. The control diagram of the proposed Duty-MPTC

The flowchart of the proposed method in one sampling time has been presented in Fig. 4.

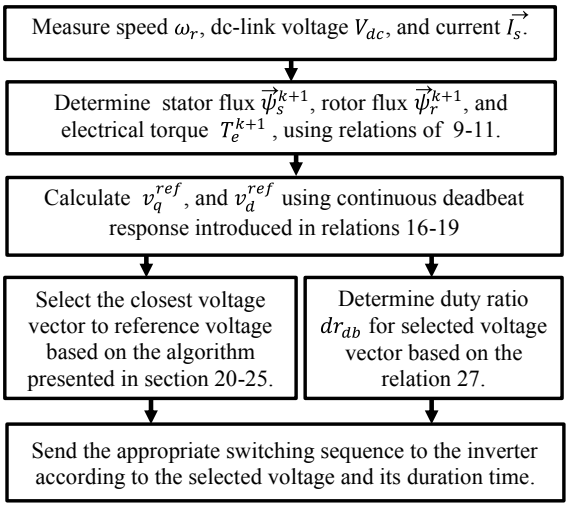

Fig. 4. Flowchart of the proposed method

4. SIMULATION STUDY

The validity of the proposed control trajectory is proven by MATLAB simulations. The proposed method includes two ideas employing both one and two voltage vectors in any control cycle. In the case of the one voltage-vector-based methods, the simulations are done for the proposed method and the MPTC presented in [7]. Also, in the case of the two-vector-based method, our MPTC with the duty cycle and the duty-cycle-based MPTC investigated in [23] is simulated. To simplify, the proposed MPTC, the MPTC presented in [7], the proposed MPTC with duty cycle, and the duty-cycle-based MPTC investigated in [23] are called MPTC-I, MPTC-II, Duty-MPTC-I, and Duty-MPTC-II, respectively. The sampling time of all simulations has been set to 80 µs. Thus, the switching frequencies in one-vector-based techniques for identified speeds are the

same and vary with respect to speed. But, in the duty-cycle-based algorithms, average switching frequencies are around 16.66 Kh. Therefore, comparisons are fair. Both motor and system parameters have been presented in Table 1.

Table 1
Motor and control system parameters

Parameters	Values	Parameters	Values
R_s	10.8 Ω	P_{out}	0.75 kW
R_r	15 Ω	T_{rated}	4 Nm
L_s	0.477 H	f	50 Hz
L_r	0.477 H	ψ_s^{ref}	0.87 Wb
L_m	0.435 H	V_{dc}	540 V
P	4	J	0.000152 kgm^2

Meanwhile, the Torque ripple and flux ripples indexes are root-mean squares of the torque and flux deviations with respect to their commanded values.

In the first simulation test, the steady-state operation of the four aforementioned methods has been simulated and the respective results are depicted in Figs. 5–8.

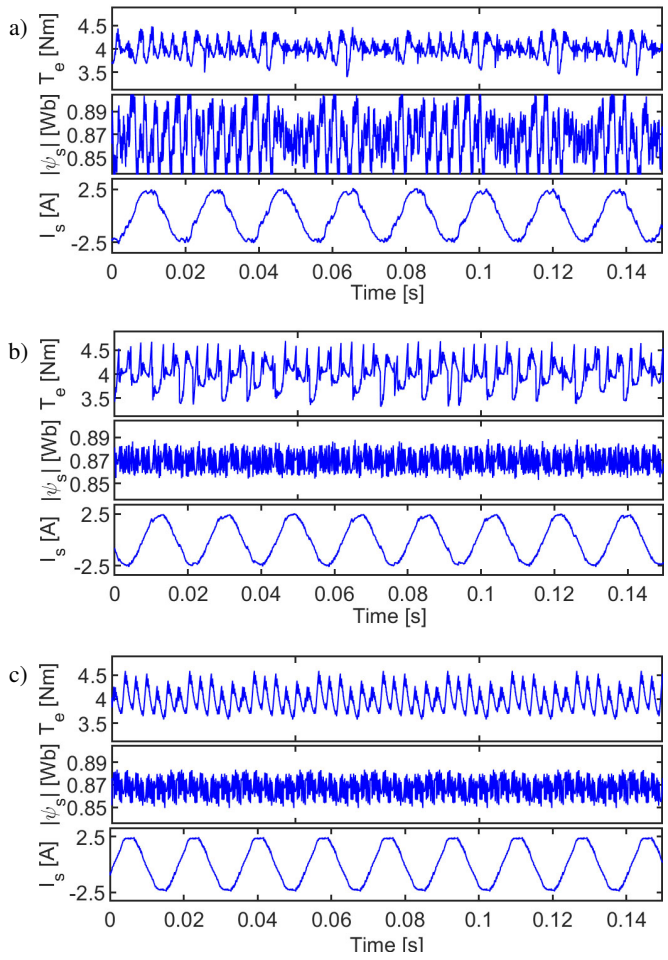

Fig. 5. Simulated steady-state response at 1500 rpm with rated torque (4 Nm): a) MPTC-I with weighting factor 100; b) MPTC-I with weighting factor 18.4; c) MPTC-II

Figures 5 and 6 show the results of MPTC$_\tau$ and MPTC$_\tau$I at low and high speeds. Figures 5a, and 5b present the results of MPTC-I with weighting factor 18.4 presented in [9] and weighting factor 100, respectively. In Fig. 5a, the torque ripple is 0.045, which is lower than 0.074 presented in Fig. 5b, and conversely, in Fig. 5a, the relative flux ripples are 0.022, which is greater than 0.009 presented in Fig. 5b. However, as can be observed, in the MPTC$_\tau$I, due to comparing reference voltage with feasible voltage vectors, the torque and flux ripples are 0.057 and 0.0094, respectively, which means an accurate compromise is provided between both the torque and flux ripples.

Similarly, in low-speed performance, for MPTC$_\tau$ with the weighting factor of 18.4, MPTC$_\tau$ with the weighting factor of 100, and MPTC$_\tau$I, the relative torque ripples are 0.051, 0.062, and 0.057, respectively. Meanwhile, the current waveforms have THDs equalling 0.066, 0.062, and 0.056 for the previous aforementioned methods, respectively. These values verify that MPTC$_\tau$I has the lowest THD value among the three other methods. The related results are shown in Fig. 6.

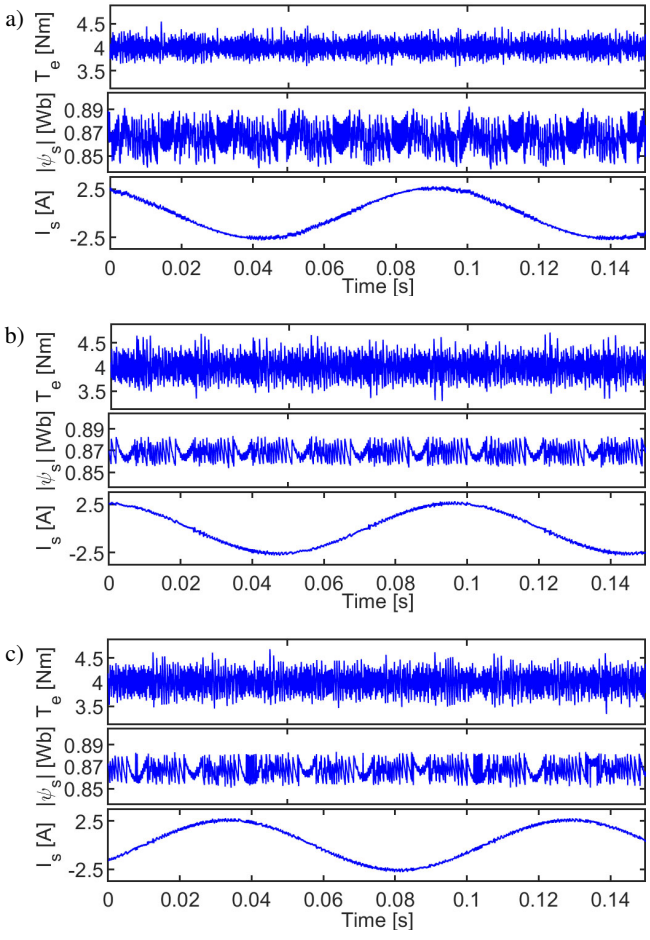

Fig. 6. Simulated steady-state response at 150 rpm with rated torque (4 Nm): a) MPTC-I with weighting factor 18.4; b) MPTC-I with weighting factor 100; c) MPTC-II

Also, the steady state operation of duty-cycle-based methods at low speed has been shown in Figs. 7 and 8. The relative torque ripples in the Duty-MPTC-I for weighting factors 20

and 100 are 0.051 and 0.062, respectively. Also, for this method with the mentioned weighting factors, flux ripples are 0.014 and 0.0077, respectively. In Duty-MPTC-I with the weighting factor of 100, due to the priority of torque error term, the torque ripple is lower than that of duty-MPTC-I with the weighting factor of 18.4. This issue in the case of flux ripple is different. However, in Duty-MPTC-II due to the equal importance of torque and flux tracking, the compromise between the torque and flux ripple has been observed.

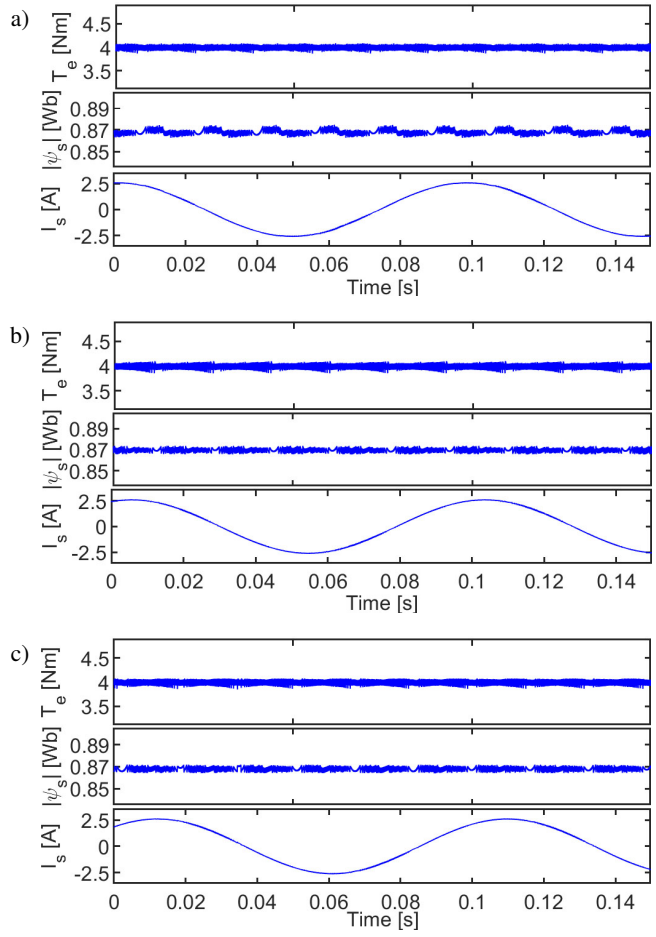

Fig. 7. Simulated steady-state response at 150 rpm with rated torque (4 Nm): a) Duty-MPTC-I with weighting factor 18.4; b) Duty-MPTC-I with weighting factor 100; c) Duty-MPTC-II

The conclusion performed at low speed is applied to high-speed performance and it is not repeated here. However, the related curves have been shown in Fig. 8. and quantitative results have been presented in Table 2.

Transient tests of MPTC-I, MPTC-II, Duty-MPTC-I, and Duty-MPTC-II in the maneuver of exerting load torque step have been conducted and shown in Figs. 9 and 10.

Since the fastest transient response of the electrical torque is achieved by considering a low value of the weighting factor, in this section only the weighting factor of 100 has been studied for MPTC-I and Duty-MPTC-I. As shown in Figs. 9 and 10 firstly, the motor runs at 1500 rpm, then at time instant 0.05s a mechanical load of 4 Nm is exerted to the shaft of the

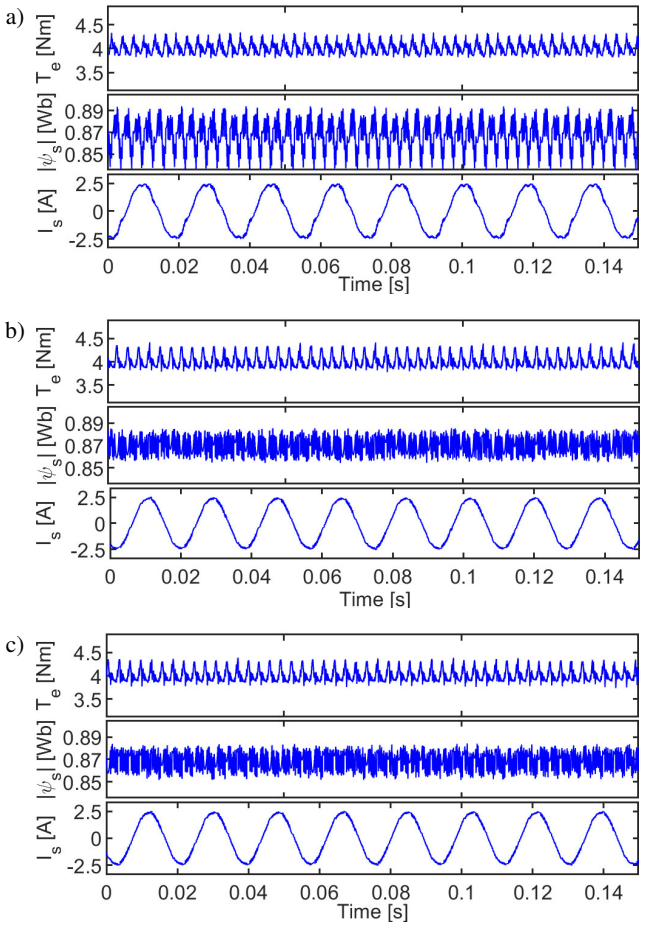

Fig. 8. Simulated steady-state response at 1500 rpm with rated torque (4 Nm): a) Duty-MPTC-I with weighting factor 18.4; b) Duty-MPTC-I with weighting factor 100; c) Duty-MPTC-II

Table 2
Simulated results at 1500 rpm with 4 Nm load

Method	$T_{e-rip}(\%)$	$\psi_{s-rip}(\%)$	$THD\ (\%)$
Duty-MPTC-I WF = 100	2.9	1.5	5
Duty-MPTC-I WF = 18.4	3.4	0.89	5.8
Duty-MPTC-II	3.2	0.9	6.9

motor. For all of the understudied techniques, it takes around 2 Ms until the torque tracks its nominal value. Also, during this sudden load change, the stator flux remains constant, which confirms that the proposed method satisfies an appropriate dynamic response of the torque and a decoupled control of the torque and flux.

Finally, peed reversal performance at low speed has been shown in Fig. 11. It can be seen that the no load motor deaccelerates rapidly from 150 to 0 rpm and then accelerates to −150 rpm. During the change of speed, the stator flux amplitude remains constant. This simulation confirms the decouple control of the flux and torque over low-speed ranges. Also, this figure shows that the level of ripples at low speed at no load state is extremely low.

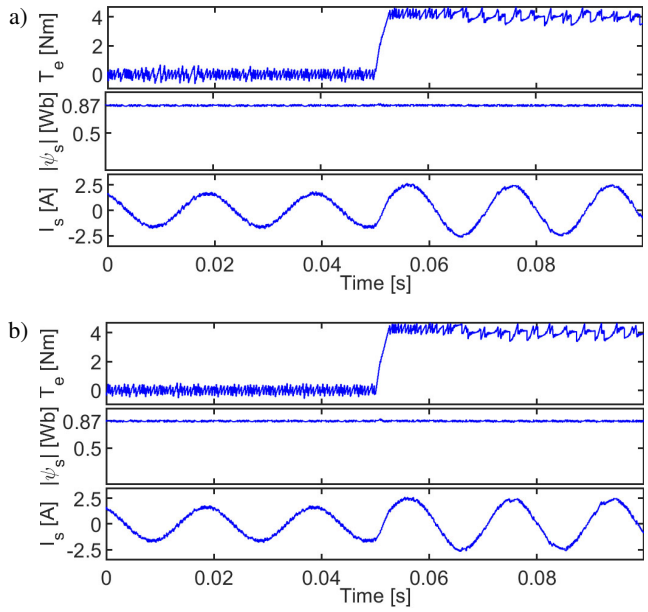

Fig. 9. Simulated dynamic operation at 1500 rpm under load torque step (4 Nm): a) MPTC-I and b) MPTC-II

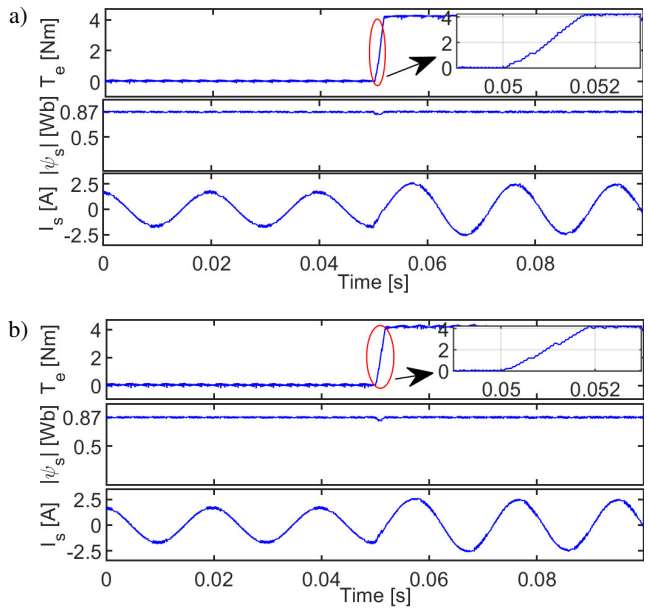

Fig. 10. Simulated dynamic operation at 1500 rpm with abrupt load change (4 Nm): a) Duty-MPTC-I and b) Duty-MPTC-II

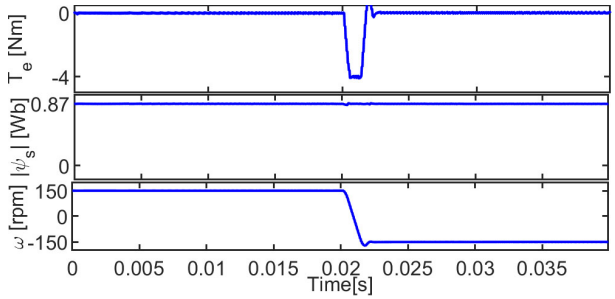

Fig. 11. Simulation of low-speed reversal operation at 150 rpm for Duty-MPTC-II

5. EXPERIMENTAL RESULTS

In this part, to verify the simulation results of the understudy methods, several related experiments have been conducted on a test bench. The machine parameters and reference values are the same as those tabulated in Table 1. Launchpad XL TMS320F28379D, 200 MHz, and floating-point DSP board are used to implement the aforementioned strategies coded through Simulink in MATLAB software. The control period of the practical tests has been fixed at 12.5 kHz. Figure 12 shows the employed platform.

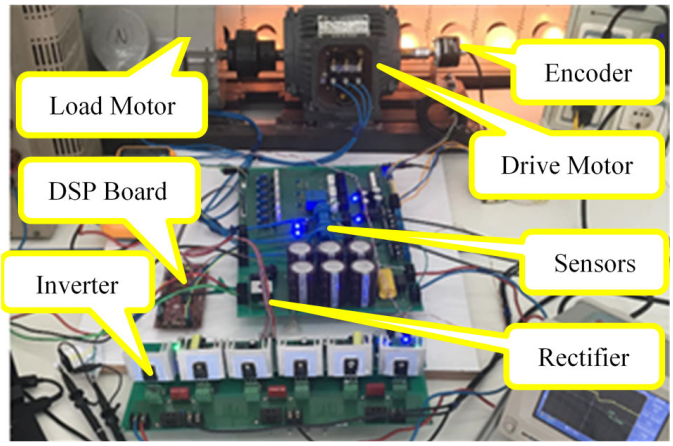

Fig. 12. Test bench of control system

Steady state operation is the first test analysed in this section. The motor rotates at 1500 r/min with 4 Nm mechanical torque. Respective waveforms are depicted in Figs. 13 and 14. Also, the ripples of electrical torque and stator flux, as well as the

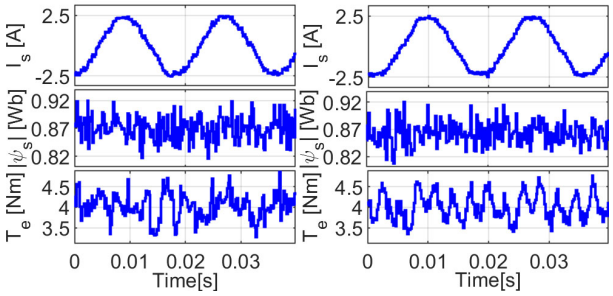

Fig. 13. Experimental steady-state responses at 1500 rpm with nominal load: left MPTC-I and right MPTC-II

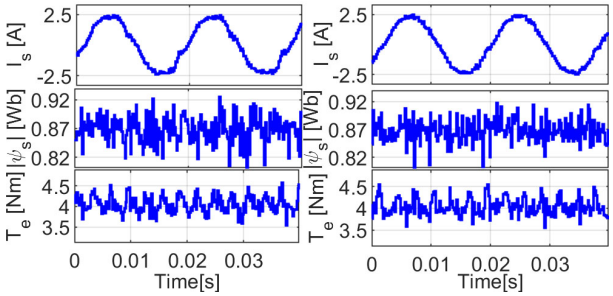

Fig. 14. Experimental steady-state responses at 1500 rpm with nominal load: left Duty-MPTC-I and right Duty-MPTC-II

current THD, are shown in Tables 3 and 4. Due to page limitations, MPTC-I and Duty-MPTC-I have been presented with only weighting factors of 100 and 18.4, respectively.

Table 3
Simulated results at 1500 rpm with 4 Nm load

Method	T_{e-rip} (%)	ψ_{s-rip} (%)	THD (%)
MPTC-I WF = 100	7.5	2.4	9.2
MPTC-II	7.6	1.8	8.8

Table 4
Simulated results at 1500 rpm with 4 Nm load

Method	T_{e-rip} (%)	ψ_{s-rip} (%)	THD (%)
Duty-MPTC-I WF = 18.4	4.9	1.9	8.5
Duty-MPTC-II	4.9	1.5	6.9

As shown in Figs. 13 and 14, in MPTC-II and Duty-MPTC-II, the compromise between the torque deviation and deviation error is well satisfied. But in MPTC-I and Duty-MPTC-II due to the importance of the torque or stator flux determined with weighting factors, either the torque or flux error can be lower.

In this condition, the machine rotates at rated speed without load. Then, the rated torque is suddenly exerted on the motor shaft. The curves of the nominal load disturbance explicit that variables in MPTC-II and Duty-MPTC-II quickly follow the reference values, similar to MPTC-I and Duty-MPTC-I. As shown in Figs. 15 and 16 after exerting the mechanical load, the mechanical speed declined to around 1285 rpm and rapidly returned to the command values.

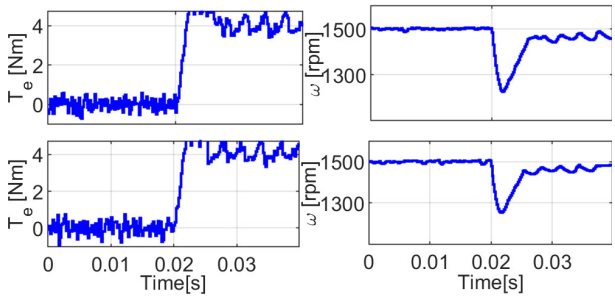

Fig. 15. Experimental results under load torque step (4 Nm) left MPTC-I and right MPTC-II

The short execution time of the algorithm is another advantage of the proposed method, which is investigated in this section. The results related to the execution time of different MPTC-based algorithms are given in Table 5. In algorithms based on predictive control, the execution time is relatively high, and the reason is the prediction phase, which must be performed to the number of candidate voltage vectors. Thus, reducing the candidate voltage vectors can significantly reduce the execution time of the prediction stage, and the total execution time of the whole algorithm is reduced. As the prediction

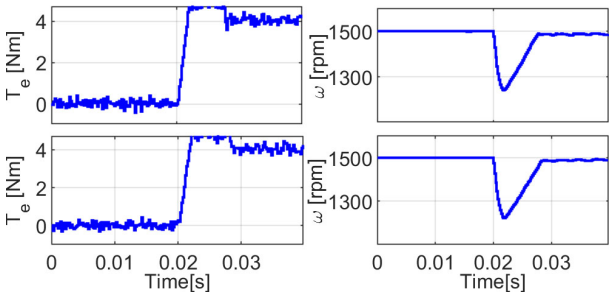

Fig. 16. Experimental results under load torque step (4 Nm) left Duty-MPTC-I and right Duty-MPTC-II

operations in the proposed method are performed only once, the execution time is significantly reduced. Also, in many methods, reducing the number of candidate voltage vectors requires determining the stator flux position which itself requires a high computational time, while in the proposed method, it is not necessary to determine the position of the stator flux. This case also has a major contribution to reducing the execution time of the proposed algorithm.

Table 5
Comparison the execution time of different algorithms

Execution time	MPTC[16] (μs)	MPTC[9] (μs)	MPTC[14] (μs)	MPTCII (μs)
Measurement	2.15	2.15	2.15	2.15
Observation	4.18	4.18	4.18	4.18
Flux position	0	0	1.24	0
VV selection	1.1	0	1	0
Prediction	3.1	9.1	3	1.5
Optimization	1.2	4	1	1
Total	**11.73**	**19.43**	**12.57**	**8.83**

6. CONCLUSIONS

Performing a large number of predictions is the major drawback of FCS-MPTC. By making only one prediction, not only computational burden of FCS-MPTC is decreased, but also, by helping to obtain an optimum voltage vector, the duty cycle is calculated to reduce the ripples of the variable. Along with this strategy, another important advantage is achieved. This benefit is the use of simple relationships instead of cost function calculation and its evaluation. Using these relationships relieves MPTC from the weighting factor tunning problem and provides a good compromise between the torque error and flux error. The major results deduced from the proposed algorithm are given as follows:

- The direct selection of optimum voltage vector removes the challenge of cost function employment as well as weighting factor tunning.
- The ratio of reference voltage over the magnitude of basic voltage vectors achieves an appropriate duty cycle without using any complicated analysis and further calculations.

- Prediction operations are not repeated for all feasible voltage vectors and are performed only one time to calculate the optimum virtual voltage vector.
- Although a continuous voltage vector is employed to control processes, the rotary to stationary transformation is not required.
- Since an optimum voltage vector and its respective duty ratio are determined based on both the torque and flux responses, both the torque and flux ripples are reduced compromisingly.
- Since the computational burden of the proposed algorithm is reduced in the prediction and voltage vector selection stages, as well as the duty ratio determination stage, the total execution time of the proposed method is decreased.

Both the simulation and experimental tests have transparently verified the excellent performance of the proposed method.

REFERENCES

[1] D. Stando and M.P. Kazmierkowski, "Constant switching frequency predictive control scheme for three-level inverter-fed sensorless induction motor drive," *Bull. Pol. Acad. Sci. Tech. Sci.*, vol. 68, no. 5, pp. 1057–1068, 2020, doi: 10.24425/bpasts.2020.134668.

[2] V. Talavat, S. Galvani, and M. Hajibeigy, "Direct predictive control of asynchronous machine torque using matrix converter," *Arch. Electr. Eng.*, vol. 67, no. 4, pp. 773–788, 2018, doi: 10.24425/aee.2018.124739.

[3] R. Narayan and D.B. Subudhi, "Stator inter-turn fault detection of an induction motor using neuro-fuzzy techniques," *Arch. Control Sci.*, vol. 20, no. 3, pp. 363–376, 2010, doi: 10.2478/v10170-010-0022-7.

[4] J. Rodriguez *et al.*, "State of the art of finite control set model predictive control in power electronics," *IEEE Trans. Ind. Inform.*, vol. 9, no. 2, pp. 1003–1016, May 2013, doi: 10.1109/TII.2012.2221469.

[5] S.A. Davari, D.A. Khaburi, and R. Kennel, "An improved FCS-MPC algorithm for an induction motor with an imposed optimized weighting factor," *IEEE Trans. Power Electron.*, vol. 27, no. 3, pp. 1540–1551, Mar. 1981, doi: 10.1109/TPEL.2011.2162343.

[6] T. Vyncke, S. Thielemans, T. Dierickx, R. Dewitte, M. Jacxsens, and J. Melkebeek, "Design choices for the prediction and optimization stage of finite-set model predictive control," in *Proc. 2011 Workshop on Predictive Control of Electrical Drives and Power Electronics*, 2011, pp. 47–54, doi: 10.1109/PRECEDE.2011.6078687.

[7] J. Rodriguez, R.M. Kennel, J.R. Espinoza, M. Trincado, C.A. Silva, and C.A. Rojas, "High performance control strategies for electrical drives: An experimental assessment," *IEEE Trans. Ind. Electron.*, vol. 59, no. 2, pp. 812–820, Feb. 2012, doi: 10.1109/TIE.2011.2158778.

[8] C.A. Rojas, J. Rodriguez, F. Villarroel, J.R. Espinoza, C.A. Silva, and M. Trincado, "Predictive torque and flux control without weighting factors," *IEEE Trans. Ind. Electron.*, vol. 60, no. 2, pp. 680–690, Feb. 2013, doi: 10.1109/TIE.2012.2206344.

[9] M. Norambuena, J. Rodriguez, Z. Zhang, F. Wang, C. Garcia, and R. Kennel, "A very simple strategy for high-quality performance of AC machines using model predictive control," *IEEE Trans. Power Electron.*, vol. 34, no. 1, pp. 794–800, Jan. 2019, doi: 10.1109/TPEL.2018.2812833.

[10] Y. Zhang, B. Zhang, H. Yang, M. Norambuena, and M.J. Rodriguez, "Generalized sequential model predictive control of IM drives with field-weakening ability," *IEEE Trans. Power Electron.*, vol. 34, no. 9, pp. 8944–8955, Sept. 2019, doi: 10.1109/TPEL.2018.2886206.

[11] M.R. Nikzad, B. Asaei, and S.O. Ahmadi. "Discrete duty-cycle-control method for direct torque control of induction motor drives with model predictive solution," *IEEE Trans. Power Electron.*, vol. 33, no. 3, pp. 2317–2329, Mar. 2018, doi: 10.1109/TPEL.2017.2690304.

[12] F. Wang, S. Li, X. Mei, W. Xie, J. Rodríguez, and R. Kennel, "Model-based predictive direct control strategies for electrical drives: An experimental evaluation of PTC and PCC methods," *IEEE Trans. Ind. Inform.*, vol. 11, no. 3, pp. 671–681, Jun. 2015, doi: 10.1109/TII.2015.2423154.

[13] Y. Zhang, H. Yang, and B. Xia, "Model-predictive control of induction motor drives: Torque control versus flux control," *IEEE Transactions on Ind. App.*, vol. 52, no. 5, pp. 4050–4060, Sep. 2016, doi: 10.1109/TIA.2016.2582796.

[14] M. Habibullah, D.D. Lu, D. Xiao, and M.F. Rahman, "A simplified finite-state predictive direct torque control for induction motor drive," *IEEE Trans. Ind. Electron.*, vol. 63, no. 6, pp. 3964–3975, Jun. 2016, doi: 10.1109/TIE.2016.2519327.

[15] W. Xie *et al.*, "Finite-control-set model predictive torque control with a deadbeat solution for PMSM drives," *IEEE Trans. Ind. Electron.*, vol. 62, no. 9, pp. 5402–5410, Sep. 2015, doi: 10.1109/TIE.2015.2410767.

[16] M. Mamdouh and M.A. Abido, "Efficient predictive torque control for induction motor drive," *IEEE Trans. Ind. Electron.*, vol. 69, no. 9, pp. 6757–6767, Sep. 2019, doi: 10.1109/TIE.2018.2879283.

[17] Y. Zhang and J. Zhu, "Direct torque control of permanent magnet synchronous motor with a reduced torque ripple and commutation frequency," *IEEE Trans. Power Electron.*, vol. 26, no. 1, pp. 235–248, Jan. 2011, doi: 10.1109/TPEL.2010.2059047.

[18] Y. Ren, Z.Q. Zhu, and J. Liu, "Direct torque control of permanent-magnet synchronous machine drives with a simple duty ratio regulator," *IEEE Trans. Ind. Electron.*, vol. 61, no. 10, pp. 5249–5259, Oct. 2014, doi: 10.1109/TIE.2014.2300070.

[19] Q. Liu and K. Hameyer, "Torque ripple minimization for direct torque control of PMSM with modified FSMPC," *IEEE Trans. Ind. Electron.*, vol. 52, no. 6, pp. 4855–4864, Dec. 2016, doi: 10.1109/TIA.2016.2599902.

[20] L. Rovere, A. Formentini, A. Geaeta, P. Zanchetta, and M. Marchesoni, "Sensorless finite control set model predictive control for IPMSM drives," *IEEE Trans. Power Electron.*, vol. 63, no. 9, pp. 5921–5931, Sep. 2016, doi: 10.1109/TIE.2016.257 8281.

[21] Y. Zhang, H. Yang, and B. Xia, "Model predictive torque control of induction motor drives with reduced torque ripple," *IET Electr. Power Appl.*, vol. 9, no. 9, pp. 595–604, 2015, doi: 10.1049/iet-epa.2015.0138.

[22] Y. Zhang and H. Yang, "Model predictive flux control of induction motor drives with switching instant optimization," *IEEE Trans. Energy Convers.*, vol. 30, no. 3, pp. 1113–1122, Sep. 2015, doi: 10.1109/TEC.2015.2423692.

[23] Y. Zhang and H. Yang, "Model predictive torque control of induction motor drives with optimal duty cycle control," *IEEE Trans. Power Electron.*, vol. 29, no. 12, pp. 6593–6603, Dec. 2014, doi: 10.1109/TPEL.2014.2302838.

[24] Y. Zhang and H. Yang, "Generalized two-vector-based Model-predictive torque control of induction motor drives," *IEEE Trans. Power Electron.*, vol. 30, no. 7, pp. 3818–3829, July 2015, doi: 10.1109/TPEL.2014.2349508.

[25] X. Wang and D. Sun, "Three-vector-based low-complexity model predictive direct power control strategy for doubly fed induction generators," *IEEE Trans. Power Electron.*, vol. 32, no. 1, pp. 773–782, Jan. 2017, doi: 10.1109/TPEL.2016.2532387.

[26] S. Kang, J. Soh, and R. Kim, "Symmetrical three-vector-based model predictive control with deadbeat solution for IPMSM in rotating reference frame," *IEEE Trans. Ind. Electron.*, vol. 67, no. 1, pp. 159–168, Jan. 2020, doi: 10.1109/TIE.2018.2890490.

[27] B. Kiani, B. Mozafari, S. Soleymani, and H. Mohammadnezhad Shourkaei, "Predictive torque control of induction motor drive with reduction of torque and flux ripple," *Bull. Pol. Acad. Sci. Tech. Sci.*, vol. 69, no. 4, p. e137727, 2021, doi: 10.24425/bpasts.2021.137727.

[28] B. Kenny and R. Lorenz, "Stator- and rotor-flux-based deadbeat direct torque control of induction machines," *IEEE Trans. Ind. Appl.*, vol. 39, no. 4, pp. 1093–1101, Jul. 2003, doi: 10.1109/TIA.2003.813727.